Published for SISSA by Springer

Received: October 20, 2023
Revised: February 26, 2024
Accepted: February 27, 2024
Published: March 21, 2024

Gravitational self force from scattering amplitudes in curved space

Dimitrios Kosmopoulos[a] **and Mikhail P. Solon**[b]

[a]*Département de Physique Théorique, Université de Genève, 24 quai E. Ansermet, CH-1211 Geneva, Switzerland*
[b]*Mani L. Bhaumik Institute for Theoretical Physics, Department of Physics and Astronomy, University of California Los Angeles, Los Angeles, CA 90095, U.S.A.*

E-mail: dimitrios.kosmopoulos@unige.ch, solon@physics.ucla.edu

Abstract: We employ scattering amplitudes in curved space to model the dynamics of a light probe particle with mass m orbiting in the background spacetime induced by a heavy gravitational source with mass M. Observables are organized as an expansion in m/M to all orders in G — the gravitational self-force expansion. An essential component of our analysis is the backreaction of the heavy source which we capture by including the associated light degrees of freedom. As illustration we consider a Schwarzschild background and verify geodesic motion as well as the first-order self-force correction to two-body scattering through $\mathcal{O}(G^3)$. Amplitudes in curved space offer several advantages, and further developments along these lines may advance the computation of gravitational-wave signals for extreme-mass-ratio inspirals.

Keywords: Black Holes, Effective Field Theories, Nonperturbative Effects, Scattering Amplitudes

ArXiv ePrint: 2308.15304

https://doi.org/10.1007/JHEP03(2024)125

Contents

1 Introduction

The breakthrough discovery of gravitational waves [1] has catalyzed rapid progress and new directions in many areas of astronomy, cosmology, and particle physics. In theoretical high-energy physics, the challenge of modeling binary sources to high precision has inspired new methods of calculation using the tools of Quantum Field Theory (QFT), leading to a number of new results in General Relativity. In turn, the application of QFT in this new arena has uncovered theoretical structures that have brought new insights into the deep connections between field theory and Einstein's geometric picture of gravity. See, e.g., refs. [2–5] for reviews.

The QFT-based approach to classical binary dynamics weaves together cutting-edge tools from the theory of elementary particles, such as effective field theory (EFT), on-shell methods, and techniques for multi-loop integration. These tools have been honed over decades to tackle significant problems in gauge theory where multiple scales are nonlinearly coupled. However, the precision demands of future gravitational wave detectors, such as LISA [6], the Einstein Telescope [7] and Cosmic Explorer [8], are posing new challenges that will take these technologies to their breaking-point.

JHEP03(2024)125

State-of-the-art calculations provide a stress test for our understanding of QFT and unveil deep insights and underlying structure. A celebrated example is the double copy [9–11], which, in its original incarnation, directly connected amplitudes in gauge and gravitational theories, and has since been generalized to a web of interconnected theories (see ref. [12] for a recent review). Computations relevant for the binary problem, in particular, have also led to formal developments. For example, ref. [13] obtained an all-orders-in-G amplitude in the probe limit, ref. [14] exposed relations among various amplitudes in the classical limit, while ref. [15] conjectured an exponential form for the amplitude in terms of the classical radial action. These calculations demonstrate how fertile this program is for deepening our understanding of scattering amplitudes, which are some of the fundamental objects in QFT, and at the same time impacting the exciting frontier of gravitational-wave science.

In the present work we extend the application of QFT methods to binary dynamics by exploring scattering amplitudes in curved space. We leverage exact solutions to Einstein's equations to develop a framework for systematically computing classes of contributions to all orders in the gravitational coupling G but as an expansion in the small ratio of masses, $m/M \ll 1$, which characterizes so-called extreme-mass-ratio inspirals. More broadly, describing the dynamics around a non-trivial background is a rich, albeit underexplored, field-theory problem with generic aspects that can find applicability beyond the context of gravitational waves.

In attempting to address the binary inspiral problem analytically one is immediately led to the principles of EFT. Indeed, the separation of scales inherent in the problem, namely the distance between the two bodies in the inspiral phase being much larger than their size, allows one to treat the bodies as point particles. This line of reasoning led to the original treatment of the binary as two point particles following geodesics in a metric induced by their motion (see ref. [16] for a review). Later, the problem was reformulated explicitly as an EFT [17] (see also the reviews [18, 19]). The same point of view is built into the modern QFT approaches to the problem as well (see refs. [15, 20–25] for remarkable recent results at 4PM[1]).

The above approaches do not assume a hierarchy between the masses of the bodies in the binary, rather they are perturbation schemes in Newton's constant G. Indeed, one of the open challenges is modeling the inspiral of binary systems consisting of a compact body of mass m and a supermassive black hole of mass M, with $M \gg m$. The limiting case of these so-called extreme-mass-ratio inspirals is described by geodesic motion in a background spacetime, such as Schwarzschild or Kerr, but beyond this the probe particle interacts with its own gravitational field, giving rise to an effective "self-force." The gravitational self-force framework aims to solve this system as an expansion in m/M but to all orders in G. In this framework, the nth order self-force (nSF) correction is suppressed by a factor of $(m/M)^n$ when compared to geodesic motion.

Developing a systematic framework for controlled calculations of m/M corrections to binary dynamics is quite challenging. At 1SF, refs. [26, 27] obtained an equation of motion for a point particle interacting with its own gravitational field. The framework was further formalized in refs. [28–31] and extended to 2SF order in refs. [32–35] (see also [36–39]). Corrections at 2SF order will be relevant for LISA [40–42]. Current state-of-the-art

[1]The post-Minkowskian (PM) expansion is organized in powers of G: $n\text{PM} \leftrightarrow \mathcal{O}\left(G^n\right)$.

JHEP03(2024)125

computations include observables for eccentric orbits at 1SF [43, 44] and waveforms for quasicircilar orbits at 2SF [45]. There is also recent interest in studying SF corrections for scattering trajectories [46–48]. The worldline-based approach of ref. [39] extended the pioneering work of Goldberger and Rothstein [17] to curved space, and the framework we develop here shares some of its features. However, our framework is based on QFT, which has its own merits and challenges. For example, one key difference is the focus on calculating scattering amplitudes, as opposed to deriving corrections to equations of motion.

There exists many interesting connections between exact curved spacetimes and amplitudes around flat space. Indeed, by resumming Feynman diagrams [49] or using on-shell methods [50], one may relate an appropriate scattering amplitude directly to the Schwarzschild metric. Refs. [51, 52] and [53] followed an analogous approach for the Schwarzschild-Tangherlini and Reissner-Nordström-Tangherlini metrics respectively. Similarly, there is growing evidence that amplitudes of spinning particles capture observables related to the Kerr black hole [54–70]. Moreoever, amplitudes containing all-orders-in-G information have been extracted from calculations in curved space [71–77].

In this paper, we combine elements of EFT and scattering amplitudes in curved space to develop a framework for computing gravitational self-force corrections to classical binary dynamics. By expanding around the black-hole geometry sourced by the heavy particle, our interaction vertices contain information to all orders in G, and observables are organized as an expansion in powers of m/M. The dynamics of the probe particle are derived from the classical limit of self-energy diagrams of a massive scalar (see figure 5), which may be thought of as a manifestation of the fact that self-force corrections are due to the particle interacting with its own gravitational field.

An important aspect of our framework is the backreaction of the background spacetime, which we capture via light degrees of freedom that follow from symmetry breaking considerations [78–80]. In particular, the spontaneous breaking of spacetime symmetries due to the black-hole geometry dictates the existence of Goldstone bosons, which become relevant beyond the geodesic limit. This line of analysis is based solely on aspects of symmetry in QFT and leads us to incorporate effective degrees of freedom that are consistent with the worldline approach [17].

Our framework is an analytic perturbative scheme designed to leverage the all-orders-in-G information encoded in the background geometry, while still taking advantage of the efficient tools developed for flat-space calculations. Scattering amplitudes in curved space encode binary dynamics of the inspiral phase. They do not capture non-perturbative effects; rather, they are constructed to match the corresponding amplitudes in flat space when expanded in G. While the focus of our work is not on reformulating the PM expansion, it is worth noting that our curved-space framework offers several advantages for computing amplitudes in flat space. For example, particular families of diagrams in flat space are automatically combined in curved space, yielding compact expressions. Moreover, higher-order loop diagrams in flat space are mapped to lower-order loop diagrams in curved space which in some cases lead to fewer integrations (see, e.g., figure 11). In fact, our formalism yields certain classes of Feynman graphs to all orders in G.

We perform a number of nontrivial checks. In particular, we calculate the 0SF two-point amplitude, which corresponds to the flat-space two-to-two amplitude, to all orders in G,

JHEP03(2024)125

finding agreement with ref. [13]. Furthermore, since our curved-space amplitudes match flat-space amplitudes at fixed order in G, we recompute the $\mathcal{O}(G^2)$ two-point amplitude and the integrand for the $\mathcal{O}(G^3)$ two-point amplitude, finding agreement with refs. [81, 82]. As building blocks to the above amplitudes we obtain the Compton amplitude and the single-graviton-emission amplitude, which also match the literature [83].

The remainder of this paper is organized as follows: in section 2 we give a summary of our formalism, and review some background material and conventions. In section 3 we use our framework to study the 0SF dynamics of a probe particle around a Schwarzschild black hole. In section 4 we introduce the backreaction of the background and obtain the Feynman rules relevant for 1SF observables, we discuss the general powercounting and we provide consistency checks. Finally, in section 5 we conclude and present possible future directions.

Note added. While this paper was at a late stage we learned of the upcoming work [84] on an effective field theory for extreme mass ratios using a curved-space worldline formalism. We thank the authors for coordinating the appearance of the manuscripts.

2 Preliminary remarks

In this section we give an overview of our setup, discuss a few aspects of QFT in curved space, and establish our conventions.

2.1 Summary of the setup

The standard approach for describing classical two-body dynamics using scattering amplitudes is to consider two massive scalar fields interacting through gravity. Here, we instead model the binary system by considering only a single scalar field but in a curved background spacetime. This captures the dynamics of a light probe particle moving around a heavy gravitational source. Moreover, we model the backreaction or recoil of the heavy source against the probe particle by including additional light degrees of freedom. These three key elements are described by the action

$$S = S_{\rm G} + S_{\rm L} + S_{\rm H}\,, \tag{2.1}$$

where the subscripts correspond to 'gravitational,' 'light' and 'heavy.'

For the gravitational part of the action we take

$$S_{\rm G} = S_{\rm EH} + S_{\rm GF}\,, \tag{2.2}$$

where $S_{\rm EH}$ is the Einstein Hilbert action and $S_{\rm GF}$ is a gauge-fixing term; for the explicit form of these terms see eq. (4.1). $S_{\rm G}$ describes the dynamics of the graviton $h_{\mu\nu}$. In particular, we define the graviton by expanding the metric as

$$g_{\mu\nu} = \bar{g}_{\mu\nu} + \kappa\, h_{\mu\nu}\,, \tag{2.3}$$

for some background metric $\bar{g}_{\mu\nu}$, which we later specify to be the Schwarzschild metric.

For the probe particle we consider a real scalar field ϕ minimally coupled to gravity,

$$S_{\rm L} = \int d^4x\sqrt{-g}\left(\frac{1}{2}g^{\mu\nu}\partial_\mu\phi\partial_\nu\phi - \frac{1}{2}m^2\phi^2\right)\,. \tag{2.4}$$

JHEP03(2024)125

Finally, $S_{\rm H}$ captures the dynamics of the light degrees of freedom associated with the backreaction of the heavy source. As we discuss in more detail in section 4.2, choosing a particular background fixes these light degrees of freedom, and $S_{\rm H}$ is the most general effective theory that describes their interactions. Restricting to the case of a Schwarzschild black hole, for the purposes of this paper it is sufficient to consider

$$S_{\rm H} = -M \int d\tau \,, \tag{2.5}$$

where M is the mass of the black hole appearing in the metric (see eqs. (2.8) and (2.9)) and τ is its proper time. The heavy-particle contribution from this action sources the background geometry $\bar{g}$ through Einstein's equations. The geodesic motion of the probe is then seen as a consequence of the curved metric rather than the exchange of gravitons between the two particles. The remaining contributions of this action, which only contribute beyond 0SF, capture the deflection of the source.

2.2 Quantum Field Theory in curved spacetime

Let us briefly comment on a few salient features of QFT in curved spacetime that are relevant for our setup. For a comprehensive treatment we refer the reader to textbooks, e.g. [85, 86].

Firstly, we restrict our analysis to stationary spacetimes, where we are able to define a Fock space similar to the one we are familiar with from flat space. In particular, given that the spacetime is static, there exists a time-like Killing vector ∂_t associated with time translations, and we can choose both our in and out Fock spaces to comprise of eigenstates of this Killing vector, i.e. states of definite energy. This means that the in and out Fock spaces share the same vacuum and that there is no spontaneous particle production. On the other hand, if the time-like vector that defines energy eigenstates in the far past was different from the one in the far future, then a single-particle in-state might have non-trivial overlap with a multiparticle out-state.

Secondly, we restrict our analysis to spacetimes that are asymptotically flat. The black-hole geometries that belong in this category are of particular interest for modeling two-body dynamics, and we focus here on the simplest case of a Schwarzschild black hole. By constructing the Fock spaces as described above, we ensure that the vacuum state reduces to the Minkowski one away from the black hole. Thus the perturbative expansion of our amplitudes matches the corresponding one in flat space.

Finally, we do not consider horizon phenomena. Black-hole geometries generically have horizons, and one might be able to extend a geometry accurate outside the horizon to one that is also valid past the horizon. Defining a vacuum state on the extended geometry results in a state that looks mixed to an asymptotic observer, given that they do not have access to the part of the state that describes the interior of the horizon. In particular, this state appears thermal such that the density matrix corresponds to a thermal average at the Hawking temperature [87, 88]. Particle detectors placed away from the black hole would register particles in this state, a phenomenon known as Hawking radiation [89].

In our analysis we are effectively removing the physics of the horizon by our choice of vacuum state, and by treating the black-hole geometry as a (resummed) perturbative expansion about flat space. It would be interesting to return to this point and extend our

JHEP03(2024)125

formalism to retain these effects. Specifically, retaining the physics of the horizon would potentially give access to non-perturbative phenomena of interest for the binary problem, such as the excitation of quasi-normal modes.

2.3 Conventions

In this subsection we collect the conventions used in this paper. We adopt $\kappa^2 = 32\pi G$. For the Riemann tensor we use

$$g^{\mu\nu}R_{\alpha\beta\gamma\nu} = \Gamma^{\mu}{}_{\alpha\gamma,\beta} - \Gamma^{\mu}{}_{\beta\gamma,\alpha} + \Gamma^{\lambda}{}_{\alpha\gamma}\Gamma^{\mu}{}_{\beta\lambda} - \Gamma^{\lambda}{}_{\beta\gamma}\Gamma^{\mu}{}_{\alpha\lambda}\,. \tag{2.6}$$

For our scattering amplitudes we use the all-incoming convention. Throughout the paper we refer to the nSF two-point amplitude in curved space, which corresponds to the nSF two-to-two amplitude in flat space, simply as the nSF amplitude. We work with a mostly-minus metric,

$$\eta_{\mu\nu} = \begin{pmatrix} 1 & 0 & 0 & 0 \\ 0 & -1 & 0 & 0 \\ 0 & 0 & -1 & 0 \\ 0 & 0 & 0 & -1 \end{pmatrix}, \qquad \eta^{\mu\nu} = \begin{pmatrix} 1 & 0 & 0 & 0 \\ 0 & -1 & 0 & 0 \\ 0 & 0 & -1 & 0 \\ 0 & 0 & 0 & -1 \end{pmatrix}. \tag{2.7}$$

We express the Schwarzschild metric in isotropic coordinates as follows:

$$\bar{g}_{\mu\nu} = \begin{pmatrix} A & 0 & 0 & 0 \\ 0 & -B & 0 & 0 \\ 0 & 0 & -B & 0 \\ 0 & 0 & 0 & -B \end{pmatrix}, \qquad \bar{g}^{\mu\nu} = \begin{pmatrix} \frac{1}{A} & 0 & 0 & 0 \\ 0 & -\frac{1}{B} & 0 & 0 \\ 0 & 0 & -\frac{1}{B} & 0 \\ 0 & 0 & 0 & -\frac{1}{B} \end{pmatrix}, \tag{2.8}$$

where

$$A = \frac{(1-a_4)^2}{(1+a_4)^2}\,, \quad B = (1+a_4)^{b_4}\,, \quad a_4 = \frac{GM}{2r}\,, \quad b_4 = 4\,. \tag{2.9}$$

The exposition given is in exactly four dimensions. When we need to regulate infinite intermediate expressions, we choose dimensional regularization where all expressions are lifted to d dimensions. In particular, the black-hole geometry is also lifted to a corresponding d-dimensional version [90]. In this case $\eta_{\mu\nu}$ and $\bar{g}_{\mu\nu}$ are diagonal $(d \times d)$ matrices of the above form, with

$$a_4 \to a_d = \frac{4\pi GM}{(d-2)\Omega_{d-2}}\frac{1}{r^{d-3}}\,, \quad b_4 \to b_d = \frac{4}{d-3}\,, \quad \Omega_{d-2} = \frac{2\pi^{(d-1)/2}}{\Gamma\left(\frac{d-1}{2}\right)}\,. \tag{2.10}$$

3 0SF: geodesic dynamics

In this section we describe the dynamics of the probe particle to all orders in G in the limit where the source is infinitely heavy, i.e., $m \ll M$. This limit is referred to as 0SF order, and describes geodesic motion where the black hole is static during the scattering process.

In the SF expansion, higher-SF orders are suppressed compared to lower-SF orders by factors of the small ratio m/M. In section 4.5 we give the precise powercounting rules for our formalism, which make the SF counting apparent. For now we simply state that to describe

JHEP03(2024)125

Figure 1. Feynman graph for the probe two-point vertex obtained from $S^{(0)}_{\text{L, int}}$ or $S^{(0)}_{\text{LY, int}}$. We depict the probe particle as a black solid line. The dot signifies the background insertion. The background injects spatial three-momentum through the vertex, such that $\boldsymbol{p}_1 + \boldsymbol{p}_2 \neq 0$.

geodesic motion we may neglect the dynamical graviton as well as the backreaction of the background, and therefore, 0SF dynamics is captured by

$$S^{(0)}_{\text{L}} \equiv S_{\text{L}}|_{g\to\bar{g}} = \int d^4x\sqrt{-\bar{g}}\left(\frac{1}{2}\bar{g}^{\mu\nu}\partial_\mu\phi\partial_\nu\phi - \frac{1}{2}m^2\phi^2\right), \tag{3.1}$$

where $S_{\text{L}} = \sum_n S^{(n)}_{\text{L}}$, with $S^{(n)}_{\text{L}}$ being exactly order n in the graviton field $h_{\mu\nu}$.

3.1 0SF amplitude at $\mathcal{O}(G)$

Before tackling 0SF to all orders in G, we first demonstrate our formalism by deriving the two-point amplitude at $\mathcal{O}(G)$. We perform all steps of the calculation explicitly, and discuss the connection to the usual flat-space four-point amplitude.

In order to use standard methods for calculating amplitudes, we need the propagators of our fields to be identical to those in flat space. We therefore identify

$$\begin{aligned}\mathcal{L}^{(0)}_{\text{L, free}} &= \frac{1}{2}\eta^{\mu\nu}\partial_\mu\phi\partial_\nu\phi - \frac{1}{2}m^2\phi^2\,,\\ \mathcal{L}^{(0)}_{\text{L, int}} &= \frac{1}{2}\left(\sqrt{-\bar{g}}\bar{g}^{\mu\nu} - \eta^{\mu\nu}\right)\partial_\mu\phi\partial_\nu\phi - \frac{1}{2}m^2\left(\sqrt{-\bar{g}} - 1\right)\phi^2\,,\end{aligned} \tag{3.2}$$

where $S^{(0)}_{\text{L}} = \int d^4x\left(\mathcal{L}^{(0)}_{\text{L,free}} + \mathcal{L}^{(0)}_{\text{L,int}}\right)$. The terms appearing in $\mathcal{L}^{(0)}_{\text{L, int}}$ vanish in the $G \to 0$ limit as well as in the $r \to \infty$ limit, which justifies identifying them as interaction vertices. On the other hand, $\mathcal{L}^{(0)}_{\text{L, free}}$ is the usual free flat-space Lagrangian for a scalar particle, which implies the propagator

$$\underset{p}{\text{———}} = \frac{i}{p^2 - m^2}\,. \tag{3.3}$$

Throughout this paper we have the $(i\epsilon)$ prescription implicit. Since we are calculating amplitudes, we choose the Feynman prescription. By splitting the Lagrangian in this manner, we have the same propagator as in flat space, and the all-orders-in-G information is encoded in the interaction vertices. A similar approach was taken in ref. [91] in the cosmological context.

In our setup, the existence of the heavy particle is captured by the interaction vertices. In particular, there is no field that creates a heavy-particle state, and thus there are no external states for the heavy particle in our amplitudes. We therefore have the heuristic map $\mathcal{A}^{\text{curved}}_n \sim \mathcal{A}^{\text{flat}}_{n+2}$ between n-point amplitudes in curved space and $(n+2)$-point amplitudes in flat space. An important part of this work focuses on exploring the details of this map.

For two-body dynamics, we are interested in the two-point amplitude for a probe particle moving in the background metric $\bar{g}$, which corresponds to the four-point flat-space amplitude between the probe and the heavy particle that sources $\bar{g}$. We obtain the two-point amplitude using the Feynman rule derived from $\mathcal{L}^{(0)}_{\text{L, int}}$ and shown in figure 1. We define

$$C^{(0)\mu\nu}_{\text{L}} = \frac{1}{2}\left(\sqrt{-\bar{g}}\bar{g}^{\mu\nu} - \eta^{\mu\nu}\right), \quad C^{(0)}_{\text{L}} = -\frac{m^2}{2}\left(\sqrt{-\bar{g}} - 1\right), \tag{3.4}$$

JHEP03(2024)125

such that,

$$\mathcal{L}^{(0)}_{\mathrm{L,\,int}} = C^{(0)\mu\nu}_{\mathrm{L}}\partial_\mu\phi\partial_\nu\phi + C^{(0)}_{\mathrm{L}}\phi^2\,. \tag{3.5}$$

In momentum space, we have

$$S^{(0)}_{\mathrm{L,\,int}} = \int d^4x\mathcal{L}^{(0)}_{\mathrm{L,\,int}} = \int \frac{d^4p}{(2\pi)^4}\frac{d^4p'}{(2\pi)^4}\frac{d^3\boldsymbol{q}}{(2\pi)^3}(2\pi)\delta\left(E+E'\right)(2\pi)^3\delta^{(3)}\left(\boldsymbol{p}+\boldsymbol{p}'+\boldsymbol{q}\right)\times \\ \tilde{\phi}(p)\tilde{\phi}(p')\left(-p_\mu p'_\nu\tilde{C}^{(0)\mu\nu}_{\mathrm{L}}(\boldsymbol{q}) + \tilde{C}^{(0)}_{\mathrm{L}}(\boldsymbol{q})\right)\,, \tag{3.6}$$

where $p=(E,\boldsymbol{p})$, $p'=(E',\boldsymbol{p}')$, and we denote functions related by a Fourier transform with a tilde. The two-point vertex respects energy conservation for the two incoming scalar lines, but spatial three-momentum is not conserved; the background inserts spatial momentum through the vertex. This agrees with the fact that the background metric respects time-translation symmetry but breaks spatial-translation symmetry (see also section 4.2).

We may now straightforwardly compute the two-point amplitude with a single insertion of the interaction vertex in figure 1. We find

$$\mathcal{A}^{\mathrm{s.in.}}_2(p_2,\boldsymbol{q}) = 2p_{2\mu}(p_{2\nu}+q_\nu)\tilde{C}^{(0)\mu\nu}_{\mathrm{L}}(\boldsymbol{q}) + 2\tilde{C}^{(0)}_{\mathrm{L}}(\boldsymbol{q})\,, \tag{3.7}$$

where $q=(0,\boldsymbol{q})$ is the momentum transfer and 's.in.' stands for 'single insertion.' As in flat space we strip off a factor of $2\pi i\,\delta\left(E_2+E_3\right)$ in defining the amplitude, noting that here we do not have three-momentum conservation and hence only have a delta function for energy conservation. While we cannot obtain $\tilde{C}^{(0)\mu\nu}_{\mathrm{L}}$ and $\tilde{C}^{(0)}_{\mathrm{L}}$ exactly, we may perform the necessary Fourier transform order by order in G. In particular, to leading order in G and in the classical limit we have

$$\mathcal{A}^{\mathrm{s.in.}}_2(p_2,\boldsymbol{q}) = \frac{8\pi GMm^2\left(1-2\gamma^2\right)}{\boldsymbol{q}^2} + \mathcal{O}\left(G^2\right)\,, \tag{3.8}$$

where $\gamma = E_2/m$. This result matches the classical flat-space $2\to2$ amplitude at $\mathcal{O}\left(G\right)$ for two scalar particles interacting via graviton exchange, evaluated in the appropriate frame (we discuss this frame choice in detail in section 4.6). Note that in order to match the flat-space amplitude with relativistic normalization for all particles, we need to multiply the curved-space amplitude with a factor of $2M$ for each background-insertion vertex.

3.2 0SF amplitude to all orders in G

We now present a novel derivation of the 0SF contribution to all orders in G by directly computing amplitudes in curved space. It is straightforward to extend the calculation described in the previous section to compute diagrams with n insertions of the two-point vertex, and then resum the infinite set of contributions as a geometric series. Here, we present an alternative approach where the complete 0SF amplitude is instead given in terms of a single-insertion diagram using a different field basis.

The idea is to perform a field redefinition such that any multi-insertion diagram gives only superclassical iteration contributions. We start from $S^{(0)}_{\mathrm{L}}$ given in eq. (3.1) and plug in the explicit form of the background metric given in eq. (2.8),

$$S^{(0)}_{\mathrm{L}} = \int d^4x\frac{B\sqrt{AB}}{2}\left(\frac{(\partial_t\phi)^2}{A} - \frac{(\nabla\phi)^2}{B} - m^2\phi^2\right)\,. \tag{3.9}$$

JHEP03(2024)125

We then perform the field redefinition

$$\phi \to \frac{\phi}{(AB)^{1/4}}\,, \tag{3.10}$$

which results in

$$\begin{aligned} S^{(0)}_{\rm L} \to S^{(0)}_{\rm LY} &= \int d^4x\, \frac{1}{2}\left(\frac{B}{A}\,(\partial_t\phi)^2 - (\nabla\phi)^2 + \left(-Bm^2 + F\right)\phi^2\right), \\ F &= -\frac{\nabla^2 A}{4A} + \frac{3(\nabla A)^2}{16A^2} - \frac{(\nabla A)\cdot(\nabla B)}{8AB} + \frac{3(\nabla B)^2}{16B^2} - \frac{\nabla^2 B}{4B}\,, \end{aligned} \tag{3.11}$$

up to total derivatives. As we see below this new action naturally yields the amplitude in the so-called Y-pole subtraction scheme [92], hence the subscript label 'LY.' Note that the field redefinition reduces to the identity in both the $G \to 0$ and the $r \to \infty$ limits, which means that it is a valid perturbative redefinition that does not change the normalization of the external states. We find that F only contributes terms with subleading scaling in the classical limit, and we drop it henceforth.

Next, we split $S^{(0)}_{\rm LY}$ into a free part and an interaction part as in eq. (3.2). The free part is the same as before. The interaction part is

$$S^{(0)}_{\rm LY,\,int} = \int d^4x\, \frac{1}{2}\left(\left(\frac{B}{A} - 1\right)(\partial_t\phi)^2 + \left(-Bm^2 + m^2\right)\phi^2\right), \tag{3.12}$$

which again results in a Feynman vertex as the one depicted in figure 1. As we noted, this two-point vertex does not impart energy to the probe particle. We may manifest this fact by Fourier transforming in time,

$$\begin{aligned} S^{(0)}_{\rm LY,\,int} = \int d^3\boldsymbol{x}\frac{dE}{2\pi}\frac{dE'}{2\pi}(2\pi)\delta(E+E')\phi(E,\boldsymbol{x})\phi(E',\boldsymbol{x})\times \\ \frac{1}{2}\left(E^2\left(\frac{B}{A} - 1\right) + \left(-Bm^2 + m^2\right)\right). \end{aligned} \tag{3.13}$$

It is straightforward to see that multiple insertions of this vertex only contribute to super-classical iterations: such contributions involve propagators of the probe particle that need to be cancelled in order to yield a classical contribution. However, the field redefinition was chosen such that the vertex is free of spatial derivatives, and thus it is impossible to get the inverse propagators required for cancellation.

We thus identify

$$\tilde{\mathcal{A}}^{\rm 0SF}_2(p_2,\boldsymbol{x}) = m^2\left(\gamma^2\left(\frac{B}{A} - 1\right) + (1 - B)\right), \tag{3.14}$$

as an off-shell position-space generating function for the complete 0SF amplitude. The 0SF amplitude in momentum space is then

$$\mathcal{A}^{\rm 0SF}_2(p_2,\boldsymbol{q}) = \left(\int \frac{d^3\boldsymbol{x}}{(2\pi)^3} e^{-i\boldsymbol{q}\cdot\boldsymbol{x}}\tilde{\mathcal{A}}^{\rm 0SF}_2(p_2,\boldsymbol{x})\right)_{\text{on shell}} + \text{iteration}\,, \tag{3.15}$$

JHEP03(2024)125

where by 'on shell' we mean that $\boldsymbol{q}$ needs to be restricted to obey $\boldsymbol{p}_2\cdot\boldsymbol{q} = -\boldsymbol{q}^2/2$ and 'iteration' denotes the superclassical iteration contributions organized in terms of Y poles [92]. The above generating function was obtained in ref. [13], and an equivalent result was obtained in ref. [93].

We may readily expand $\tilde{\mathcal{A}}_2^{0\mathrm{SF}}(p_2,\boldsymbol{x})$ to any order in G and perform the Fourier transform to obtain the classical part of $\mathcal{A}_2^{0\mathrm{SF}}(p_2,\boldsymbol{q})$ to that order. Already in position space, however, we recognize the familiar combinations of γ^2 that appear in the probe limit of the flat-space scattering amplitudes (see, e.g., eq. (9.3) of ref. [94]). To the first few orders we have,

$$\begin{aligned}\tilde{\mathcal{A}}_2^{0\mathrm{SF}}(p_2,\boldsymbol{x}) = {}& \frac{(2\gamma^2-1)\,GMm^2}{r} + \frac{3\,(5\gamma^2-1)\,G^2M^2m^2}{4r^2} \\ & + \frac{(18\gamma^2-1)\,G^3M^3m^2}{4r^3} + \frac{(129\gamma^2-1)\,G^4M^4m^2}{32r^4} + \mathcal{O}\left(G^5\right). \end{aligned} \tag{3.16}$$

3.3 Heavy expansion and geodesic expansion

We conclude this section with a brief discussion of two alternative setups for analyzing the probe particle. The first setup is the heavy expansion familiar from Heavy Quark Effective Theory [95] as well as its recent applications for the binary problem [96]. The heavy particle expansion for the real scalar field [97] representing the probe particle is

$$\phi(x) = e^{-ip\cdot x}\varphi_p(x)/\sqrt{2m} = e^{ip\cdot x}\bar{\varphi}_p(x)/\sqrt{2m}\,. \tag{3.17}$$

With this expansion, every term in the Lagrangian has definite powercounting in m since derivatives on $\varphi_p(x)$ and $\bar{\varphi}_p(x)$ are $\mathcal{O}(q)$. We expect that with an appropriate field redefinition, this heavy expansion leads to amplitudes that are directly expressed in terms of Z-poles [15, 98] instead of Y-poles.

The second setup is inspired by the first and is similar to the WKB approximation: instead of expanding around a heavy particle moving in a straight line, we expand around a heavy particle following a geodesic in curved space [99] (see also refs. [77, 100, 101]). We thus consider the following ansatz where the plane-wave factor is replaced with a semi-classical solution to the equations of motion:

$$\phi(x) = e^{-iS_p(x)}\Phi_p(x)/\sqrt{2m} = e^{iS_p(x)}\bar{\Phi}_p(x)/\sqrt{2m}\,. \tag{3.18}$$

Here we take $S_p(x)$ to be the classical on-shell action satisfying the Hamilton-Jacobi equation, along with the requirement that it reduces to a plane wave in the limit of vanishing G,

$$\bar{g}^{\mu\nu}\,\partial_\mu S_p(x)\,\partial_\nu S_p(x) = m^2 \qquad \text{and} \qquad S_p(x) \to p\cdot x \quad \text{as} \quad G\to 0\,. \tag{3.19}$$

We may iteratively compute $S_p(x)$ in terms of simple one-dimensional integrals. The explicit form to the first few orders in G is

$$\begin{aligned} S_p(x) = {}& m\left(\gamma\, t + \sqrt{\gamma^2-1}\, z\right) + \frac{mGM\,(2\gamma^2-1)\tanh^{-1}\left(\frac{z}{r}\right)}{\sqrt{\gamma^2-1}} \\ & - \frac{mG^2M^2\left(2\,(1-2\gamma^2)^2\, z - 3\,(5\gamma^4-6\gamma^2+1)\,\sqrt{r^2-z^2}\tan^{-1}\left(\frac{z}{\sqrt{r^2-z^2}}\right)\right)}{4\,(\gamma^2-1)^{3/2}\,(r^2-z^2)} \\ & + \mathcal{O}\left(G^3\right), \end{aligned} \tag{3.20}$$

JHEP03(2024)125

where we took $p_\mu = m\left(\gamma, 0, 0, \sqrt{\gamma^2-1}\right)$. The 0SF scattering angle follows from this on-shell action using standard methods of classical mechanics.

The expansion in eq. (3.18) may be useful for resumming geodesic motion and systematically calculating deviations from it. An encouraging observation is that using this expansion in the Lagrangian removes the leading-in-m term, effectively factoring out the 0SF contribution. We postpone a detailed investigation of this to future work.

4 Beyond 0SF: backreaction

Beyond 0SF, the motion of the probe perturbs spacetime, and induces a backreaction in the background metric. This backreaction is mediated by the graviton, and also involves the deflection of the heavy source. In this section we analyze these key elements, and describe the Feynman and powercounting rules necessary for computing the nSF amplitude. We apply our formalism for computing the 1SF amplitude at $\mathcal{O}(G^2)$ and $\mathcal{O}(G^3)$, providing a non-trivial consistency check of the framework developed in this paper.

4.1 Purely gravitational part of the action

The purely gravitational part of the action is given by the Einstein-Hilbert term and the gauge-fixing term:

$$\begin{aligned} S_{\rm G} = S_{\rm EH} + S_{\rm GF} &= -\frac{1}{16\pi G}\int d^4x\sqrt{-g}R + \int d^4x\sqrt{-\bar{g}}F^\mu F_\mu\,, \\ F_\mu &= \bar{\mathcal{D}}^\nu h_{\mu\nu} - \frac{1}{2}\bar{\mathcal{D}}_\mu h\,, \quad h = \bar{g}^{\alpha\beta}h_{\alpha\beta}\,, \end{aligned} \tag{4.1}$$

where $\bar{\mathcal{D}}_\mu$ is the background-metric covariant derivative, indices are raised and lowered with the background metric $\bar{g}$, and the graviton field $h_{\mu\nu}$ is defined in eq. (2.3). We emphasize that the complete graviton dynamics in curved space includes its interaction with the light degrees of freedom of the heavy source, which we describe in section 4.2.

We obtain Feynman rules from S_G by expanding the metric as in eq. (2.3). The resulting linear-order-in-h term cancels against the corresponding term in $S_{\rm H}$, as we demonstrate in section 4.3. The higher-order-in-h terms yield the propagator for h as well as interaction vertices with the background, similar to our analysis in sections 3.1 and 3.2. Note that we only need vertices with up to $(n+1)$ graviton fields for the calculation of the nSF amplitude. In particular, in this paper we explicitly consider dynamics up to 1SF order and hence only need the action to quadratic order in h:

$$\begin{aligned} \frac{\mathcal{L}_{\rm G}}{\sqrt{-\bar{g}}} = \frac{\kappa}{16\pi G}\bar{G}^{\alpha\beta}h_{\alpha\beta} - \frac{1}{4}h^{;\beta}h_{;\beta} + \frac{1}{2}h_{\alpha\beta;\gamma}h^{\alpha\beta;\gamma} \\ + \frac{1}{4}\bar{R}\left(2h^{\alpha\beta}h_{\alpha\beta} - h^2\right) + \bar{R}_{\beta\gamma}\left(h^{\beta\gamma}h - h^\gamma_\alpha h^{\alpha\beta}\right) - \bar{R}_{\alpha\gamma\beta\lambda}h^{\alpha\beta}h^{\gamma\lambda} + \mathcal{O}\left(h^3\right)\,. \end{aligned} \tag{4.2}$$

Here $S_{\rm G} = \int d^4x\mathcal{L}_{\rm G}$ and we use the shorthand $(\ldots)_{;\mu} \equiv \bar{\mathcal{D}}_\mu(\ldots)$ for the covariant derivative. The Einstein tensor, Ricci scalar, Ricci tensor and Riemann tensor are evaluated on the background metric, and are respectively denoted by $\bar{G}^{\alpha\beta}$, $\bar{R}$, $\bar{R}_{\beta\gamma}$ and $\bar{R}_{\alpha\gamma\beta\lambda}$.

We do not set the Einstein tensor, Ricci scalar and Ricci tensor to zero, despite the fact that $\bar{g}$ is eventually taken to be the Schwarzschild metric. For instance, for the linearized

JHEP03(2024)125

Schwarzschild metric, $\bar{G}^{\alpha\beta}$, $\bar{R}$ and $\bar{R}_{\beta\gamma}$ evaluate to expressions proportional to a delta function with support on the position of the black hole. These terms are on a similar footing as terms originating from $S_{\rm H}$, which also have support on the position of the black hole; see section 4.3.

4.2 Light degrees of freedom of the heavy source

To capture the backreaction of the metric we need to introduce dynamics for the light degrees of freedom of the heavy source. While the heavy source could have various light degrees of freedom, the minimum ones are those dictated by symmetry considerations. For the Schwarzschild black-hole geometry in eq. (2.8), the existence of a source at rest in the vacuum state spontaneously breaks Poincaré symmetry to rotational symmetry. The breaking of the three translation generators induces three Goldstone bosons $\zeta^i(t)$, where $i = 1, 2, 3$ and t is the time coordinate in the system defined by eq. (2.8), while the breaking of the boost generators does not induce more Goldstone bosons [78, 79]. The $\zeta^i(t)$ describe the fluctuations of the heavy source away from its original position, hence we refer to them as deflections.

The most general effective theory that captures the dynamics of the $\zeta^i(t)$ follows from the coset construction [80]. Here we only consider minimal coupling to gravity, which leads to eq. (2.5), but it is straightforward to include finite-size effects. The resulting action is that of a point particle coupled to gravity, e.g., as in ref. [17], which is intuitive given the interpretation of the $\zeta^i(t)$ as the displacement of the heavy source. Following standard manipulations (see, e.g., section 1.2 of [102]), we embed $\zeta^i(t)$ into a covariant but redundant description

$$\zeta^i(t) \to z^\mu(\tau)\,, \tag{4.3}$$

in terms of which we may trade eq. (2.5) for the einbein-gauge-fixed Polyakov form,

$$S_{\rm H} = -\frac{M}{2}\int d\tau\,(g_{\mu\nu}\dot{x}^\mu\dot{x}^\nu + 1)\,, \quad x^\mu = v^\mu\tau + z^\mu\,, \tag{4.4}$$

which is more convenient for computations. We take $v^\mu = (1, 0, 0, 0)$. In the full quantum theory, S_H also includes gauge-fixing terms related to the reparametrization invariance of the worldline, which itself is related to the redundancy introduced in eq. (4.3) (see, e.g., section 4.2 of [102]). These terms, however, are not needed for our analysis, which follows closely that of ref. [103].

The action in eq. (4.4) is ill-defined when expanding around the gravitational field sourced by the heavy particle. Indeed, the background metric has a singularity at the position of the heavy particle, which is where we evaluate the action. Expanding eq. (4.4) as in eq. (2.3) and dropping the constant term we have

$$S_{\rm H} = -\frac{M}{2}\int d\tau\,(\bar{g}_{\mu\nu}\dot{x}^\mu\dot{x}^\nu + \kappa h_{\mu\nu}\dot{x}^\mu\dot{x}^\nu)\,, \tag{4.5}$$

where $\bar{g}$ and h are evaluated at x. We define $\delta\bar{g} \equiv \bar{g} - \eta$ and isolate the divergent term as follows:

$$\begin{aligned} S_{\rm H} &= S_{\rm H,\,div} + S_{\rm H,\,fin}\,,\\ S_{\rm H,\,div} &= -\frac{M}{2}\int d\tau\,\delta\bar{g}_{\mu\nu}\dot{x}^\mu\dot{x}^\nu\,,\\ S_{\rm H,\,fin} &= -\frac{M}{2}\int d\tau\,(\eta_{\mu\nu}\dot{x}^\mu\dot{x}^\nu + \kappa h_{\mu\nu}\dot{x}^\mu\dot{x}^\nu)\,. \end{aligned} \tag{4.6}$$

JHEP03(2024)125

For our analysis, which focuses on classical contributions in the potential region, we only require the finite term $S_{\text{H, fin}}$.

Here we consider the special case of the Schwarzschild black hole, while it would be interesting to extend our analysis to the Kerr black hole. The degrees of freedom and corresponding action for a vacuum state that spontaneously breaks rotational symmetries along with translational ones have been categorized in ref. [80]. Alternatively, we could work with a worldline theory along the lines of refs. [104–106]. We postpone this analysis to future work.

4.3 Stability of the background

In this subsection we demonstrate that our background is a proper vacuum state. In other words, our field configuration solves the equations of motion, or, equivalently, the Lagrangian terms linear in the fluctuations h and z vanish.

We start with the linear-in-z terms, which arise from the first term of $S_{\text{H, fin}}$ in eq. (4.6). We have

$$S_{\text{H, fin}}\big|_{\text{linear-in-}z} = -M \int d\tau \eta_{\mu\nu} v^\mu \dot{z}^\nu \,. \tag{4.7}$$

This is a total derivative, and hence may be removed from the action.

Next, we consider the terms linear in the graviton field h. We have two contributions, one from S_{G} and one from $S_{\text{H, fin}}$:

$$\begin{aligned} S_{\text{G}}\big|_{\text{linear-in-}h} &= \int d^4x \sqrt{-\bar{g}} \left(\frac{1}{16\pi G} \bar{G}^{\mu\nu} \right) \kappa h_{\mu\nu} \,, \\ S_{\text{H, fin}}\big|_{\text{linear-in-}h} &= \int d\tau \left(-\frac{1}{2} M v^\mu v^\nu \right) \kappa h_{\mu\nu} \,. \end{aligned} \tag{4.8}$$

For the background configuration to be stable, we need these two contributions to cancel. Here we see that the Einstein tensor $\bar{G}^{\mu\nu}$ cannot be set to zero; instead, these equations hint that it should be thought of as a distribution with support at the origin. This is indeed sensible to linear order in G, while there are subtleties at higher orders [107].

In practice, to establish that the two terms in eq. (4.8) cancel at leading order in G, we need to compute tensors such as $\bar{G}^{\mu\nu}$ with support at the origin. We do this by taking their Fourier transform in dimensional regularization. For the present paper, using the linear-order-in-G background metric in S_{G} is sufficient, and we consider the stability of the background to this order only. It would also be interesting to carry out the analysis beyond this order.

4.4 Feynman rules at 1SF

We now proceed to obtain the Feynman rules relevant for the calculation of the 1SF amplitude. The Feynman rules in curved space are not more complicated than the ones in flat space even though they encode information to all orders in G.

We start by considering the graviton vertices originating in S_{G}. Similarly to our treatment in section 3, we split the action given in eq. (4.2) into a free and interacting part by isolating the flat-space limit. The free part is

$$S_{\text{G, free}} = \int d^4x \left(\frac{1}{2} \eta^{\mu\nu}\eta^{\alpha\gamma}\eta^{\beta\delta} - \frac{1}{4} \eta^{\mu\nu}\eta^{\alpha\beta}\eta^{\gamma\delta} \right) \partial_\mu h_{\alpha\beta} \partial_\nu h_{\gamma\delta} \,, \tag{4.9}$$

JHEP03(2024)125

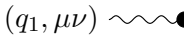

Figure 2. Feynman graph for the graviton two-point vertex obtained from $S_{\mathrm{G,\,int}}$, where the gravitons are depicted as wiggly lines. The dot signifies the background insertion. The background injects spatial momentum through the vertex, such that $\boldsymbol{q}_1 + \boldsymbol{q}_2 \neq 0$.

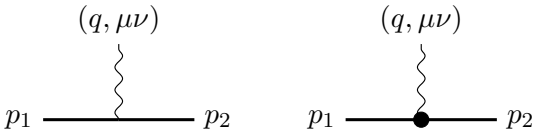

Figure 3. Feynman graphs for the probe-graviton three-point vertices obtained from $S_{\mathrm{L}}^{(1)}$ or $S_{\mathrm{LY}}^{(1)}$. The left vertex is the same as one would obtain in flat space, hence the usual momentum conservation holds. The dot on the right one signifies the background insertion. The background injects spatial momentum through the vertex, such that $\boldsymbol{p}_1 + \boldsymbol{p}_2 + \boldsymbol{q} \neq 0$. The solid black lines stand for the probe particle, while the wiggly lines stand for the graviton.

which yields the usual de Donder propagator for the graviton,

$$\mu\nu \overset{q}{\sim\sim\sim} \alpha\beta \;= \frac{i}{q^2}\mathcal{P}^{\mu\nu\alpha\beta}\,, \qquad \mathcal{P}^{\mu\nu\alpha\beta} = \frac{1}{2}\left(\eta^{\mu\alpha}\eta^{\nu\beta} + \eta^{\nu\alpha}\eta^{\mu\beta} - \eta^{\mu\nu}\eta^{\alpha\beta}\right). \tag{4.10}$$

As mentioned above, we keep the $(i\epsilon)$ prescription implicit. The interaction vertices are obtained from the remainder

$$S_{\mathrm{G,\,int}} = S_{\mathrm{G}} - S_{\mathrm{G,\,free}}\,. \tag{4.11}$$

We depict the Feynman graph for the two-point graviton vertex in figure 2.

Next, we consider the coupling of the graviton to the probe particle. We expand S_{L} as in eq. (2.3) and keep terms linear in $h_{\mu\nu}$:

$$S_{\mathrm{L}}^{(1)} = \kappa \int d^4x \sqrt{-\bar{g}}\, h^{\mu\nu}\left(-\frac{1}{2}\partial_\mu\phi\partial_\nu\phi + \frac{1}{4}\bar{g}_{\mu\nu}\bar{g}^{\alpha\beta}\partial_\alpha\phi\partial_\beta\phi - \frac{1}{4}\bar{g}_{\mu\nu}m^2\phi^2\right). \tag{4.12}$$

Here we used the notation introduced below eq. (3.1). Similar to eq. (3.11), we obtain $S_{\mathrm{LY}}^{(1)}$ via the field redefinition in eq. (3.10), and then derive the probe-graviton interaction vertex, which we depict in figure 3. For convenience, we split the vertex into the usual flat-space three-point vertex, and the remainder, which involves the background.

Finally, we consider the deflection vertices, following the treatment in ref. [103]. Again we split $S_{\mathrm{H,\,fin}}$ into a free part $S_{\mathrm{H,\,FF}}$ and an interacting part $S_{\mathrm{H,\,FI}}$:

$$S_{\mathrm{H,\,FF}} = -\frac{M}{2}\int d\tau\, \eta_{\mu\nu}\dot{z}^\mu\dot{z}^\nu\,, \quad S_{\mathrm{H,\,FI}} = S_{\mathrm{H,\,fin}} - S_{\mathrm{H,\,FF}}\,. \tag{4.13}$$

The free part gives the propagator of the deflection field,

$$\alpha \overset{\omega}{\text{- - - - - -}} \beta \;= -\frac{i}{M\omega^2}\eta^{\alpha\beta}\,, \tag{4.14}$$

where, again, based on the observable considered, one might need to keep track of the $(i\epsilon)$ prescription. From the interacting part of the action we extract the vertex sufficient for

JHEP03(2024)125

Figure 4. Feynman graph for the deflection-graviton two-point vertex obtained from $S_{\text{H, FI}}$. The dashed line stands for the deflection field, while the wiggly stands for the graviton. The vertex satisfies energy conservation: $\omega + q_0 = 0$.

computing the 1SF amplitude. In doing so, we keep in mind that the worldline Lagrangian is evaluated at x^μ given in eq. (4.4). We find

$$S_{\text{H, FI}} = -\frac{\kappa M}{2} \int d\tau \left(2h_{\mu\nu}(v\tau) v^\mu \dot{z}^\nu + h_{\mu\nu,\alpha}(v\tau) v^\mu v^\nu z^\alpha + \mathcal{O}\left(z^2\right) \right) , \tag{4.15}$$

where the graviton field is evaluated at $v^\mu \tau$. This yields the deflection-graviton vertex depicted in figure 4. Since $S_{\text{H, FI}}$ is independent of the background metric, the vertex is identical to the one of ref. [103].

4.5 Diagrams at nSF

In this subsection we discuss a few aspects of the diagrams contributing to the nSF amplitude, namely their powercounting, the required Feynman rules, and the contribution from the deflection of the heavy source.

Firstly, we note that the diagram loop counting for the two-point amplitudes in curved space coincides with the SF counting, but it is different from the number of loop integrations as we discuss below. For example, for the 0SF dynamics considered in section 3 we only have diagrams with no loops, while the 1SF amplitudes considered in this section are given by diagrams with a single loop. This is schematically shown in figure 5. A similar relation between the loop and SF counting was noted in ref. [39].

To see this, recall that in the classical limit the two-point amplitude $\mathcal{A}_2$ admits the expansion,

$$\begin{aligned} &\text{Momentum space:} && \mathcal{A}_2(\boldsymbol{q}) = \frac{Gm^2}{\boldsymbol{q}^2} \sum_{n=1}^{\infty} P_n\left(m,\, M\right) \left(G|\boldsymbol{q}|\right)^{n-1} , \\ &\text{Position space:} && \tilde{\mathcal{A}}_2(r) = m^2 \sum_{n=1}^{\infty} \tilde{P}_n\left(m,\, M\right) \left(\frac{G}{r}\right)^n , \end{aligned} \tag{4.16}$$

where P_n and $\tilde{P}_n$ are polynomials of degree n in the arguments and we keep the dependence of p_2 and γ implicit. Neglecting the deflection contribution momentarily, factors of M only appear through the background metric and only in the combination GM/r, which has classical scaling. Hence, in our formalism the amplitude is organized as

$$\tilde{\mathcal{A}}_2(r) = m^2 \sum_{n=0}^{\infty} \mathcal{F}_n[GM/r] \left(\frac{Gm}{r}\right)^n , \tag{4.17}$$

in position space and similarly in momentum space, for some functions $\mathcal{F}_n[GM/r]$ (see, e.g., eq. (3.16)). In this way, we see that powers of m are correlated to powers of G that do not originate in background insertions. In fact, the source of these factors is the probe-graviton vertices, establishing that the effective coupling constant in our theory is Gm, from which it

JHEP03(2024)125

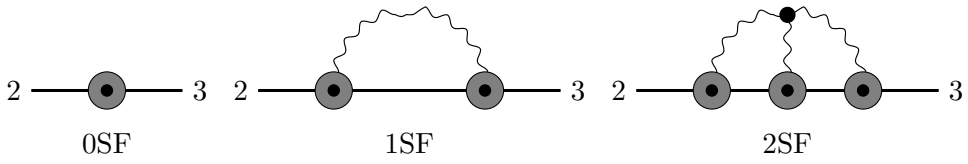

Figure 5. Schematic depiction of the diagram loop-order ↔ SF-order correspondence in our formalism. Only representative diagrams are shown. The gray blobs with the black dot denote the corresponding tree-level amplitudes where diagrams with any number of background insertions and virtual deflections have been included. The external probe-particle lines have momenta p_2 and p_3.

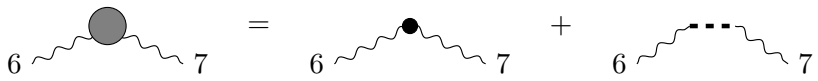

Figure 6. The Compton amplitude given as a sum of Feynman diagrams. The gray large blob stands for the on-shell amplitude, while the rest of the symbols are defined in earlier figures. The on-shell gravitons have momenta q_6 and q_7 and polarization tensors ε_6 and ε_7. We choose this labeling scheme to avoid confusion with subsequent graphs.

immediately follows that loops count the SF order, i.e. the order in m. Finally, returning to the deflection contributions, these also scale classically and contribute via the combination GM, as can be seen, e.g., in eq. (4.19), so they are on the same footing as background insertions.

We evaluate diagrams using the familiar flat-space tools, such that a diagram with l loops, n background insertions and k virtual deflections requires $l+n+k-1$ integrals. We emphasize again that the number of loops in the diagram and the number of loop integrals, while related, do not coincide in our formalism.

Secondly, we note that we only require a finite number of Feynman rules to compute diagrams at a given SF order since vertices with higher multiplicity would lead to more loops and would thus be higher SF order. In particular, at nSF, we require vertices with up to $(n+1)$ gravitons, vertices with two probe particles and up to n gravitons, and vertices with a single graviton and n deflections. In the previous subsection, we obtained the Feynman vertices sufficient for computing the 1SF amplitude.

Finally, for an analysis that focuses on the potential region for the gravitons, we only need to consider up to n virtual deflections of the heavy source at nSF. Additional deflections involve extra graviton legs that would either lead to more loops, which would be higher SF, or to contributions outside the potential region. The latter (e.g., at 1SF see bottom right diagram in figure 10) correspond to so-called mushroom diagrams in flat space where a graviton begins and ends on the same matter line.

4.6 1SF amplitude at $\mathcal{O}(G^2)$

We proceed to compute the Compton amplitude, i.e. the amplitude for the emission of two gravitons from the heavy source, and the 1SF amplitude at $\mathcal{O}(G^2)$ or 2PM. These are the simplest amplitudes where backreaction of the background enters the calculation.

For the calculation of the Compton amplitude $\mathcal{A}_{\rm C}$, where the subscript 'C' stands for 'Compton,' there are two diagrams that contribute, which we depict in figure 6. We refer to the contribution from the first diagram in figure 6 as $\mathcal{A}^{\rm b}_{\rm C}$, where 'b' stands for 'background

JHEP03(2024)125

insertion,' and the second diagram as $\mathcal{A}_{\rm C}^{\rm d}$, where 'd' stands for 'deflection.' We have,

$$\mathcal{A}_{\rm C} = \mathcal{A}_{\rm C}^{\rm b} + \mathcal{A}_{\rm C}^{\rm d}\,, \tag{4.18}$$

with

$$\begin{aligned}
\mathcal{A}_{\rm C}^{\rm b} \;=\; & -\frac{8\pi GM}{q_6\cdot q_7}\Big(\omega^2(\varepsilon_6\cdot\varepsilon_7)^2 + \big((v\cdot\varepsilon_7)(\varepsilon_6\cdot q_7) - (v\cdot\varepsilon_6)(\varepsilon_7\cdot q_6)\big)^2 \\
& + 2(\varepsilon_6\cdot\varepsilon_7)\Big((v\cdot\varepsilon_6)(v\cdot\varepsilon_7)(q_6\cdot q_7) + \omega\big((v\cdot\varepsilon_7)(\varepsilon_6\cdot q_7) - (v\cdot\varepsilon_6)(\varepsilon_7\cdot q_6)\big)\Big)\Big)\,, \\
\mathcal{A}_{\rm C}^{\rm d} \;=\; & \frac{8\pi GM}{\omega^2}(v\cdot\varepsilon_6)(v\cdot\varepsilon_7)\Big(4\omega^2(\varepsilon_6\cdot\varepsilon_7) - (v\cdot\varepsilon_6)(v\cdot\varepsilon_7)(q_6\cdot q_7) \\
& + 2\omega\big((v\cdot\varepsilon_7)(\varepsilon_6\cdot q_7) - (v\cdot\varepsilon_6)(\varepsilon_7\cdot q_6)\big)\Big)\,.
\end{aligned} \tag{4.19}$$

In the above we used

$$\omega = v\cdot q_6 = -v\cdot q_7\,, \quad \varepsilon_{6\,\mu\nu} = \varepsilon_{6\,\mu}\,\varepsilon_{6\,\nu}\,, \quad \varepsilon_{7\,\mu\nu} = \varepsilon_{7\,\mu}\,\varepsilon_{7\,\nu}\,, \tag{4.20}$$

with v defined below eq. (4.4). Combining the two contributions we arrive at the familiar result,

$$\begin{aligned}
\mathcal{A}_{\rm C} = -\frac{8\pi GM}{\omega^2(q_6\cdot q_7)}\Big(&\omega^2(\varepsilon_6\cdot\varepsilon_7) - (v\cdot\varepsilon_6)(v\cdot\varepsilon_7)(q_6\cdot q_7) \\
&+ \omega\big((v\cdot\varepsilon_7)(\varepsilon_6\cdot q_7) - (v\cdot\varepsilon_6)(\varepsilon_7\cdot q_6)\big)\Big)^2\,,
\end{aligned} \tag{4.21}$$

which manifests the double-copy structure [9–11] of the Compton amplitude. All pieces of our Compton amplitude have classical scaling, which would simplify book-keeping of classical contributions especially for higher-order processes. As mentioned above, to compare the result in eq. (4.21) to the corresponding flat-space amplitude, we divide the latter by $2M$ to account for non-relativistic normalization.

In comparing our amplitudes with corresponding flat-space ones, we should be mindful in our mapping of v to the momentum of the heavy particle. This point, while not relevant for the Compton amplitude itself, may enter in higher-order computations that involve superclassical terms. Let p_1 be the incoming momentum of the heavy particle in flat-space kinematics and q be the total momentum transfer of the process at hand (here $q = q_6 + q_7$). Since in curved space we have $v\cdot q = 0$, we may identify

$$v = \bar{p}_1/\bar{M}\,, \quad \bar{p}_1 = p_1 + \frac{1}{2}q\,, \quad \bar{M}^2 = \bar{p}_1^2\,. \tag{4.22}$$

This in turn implies that the frame in which we do our curved-space calculations corresponds to the flat-space frame in which $\bar{p}_1^\mu = (\bar{M},0,0,0)$, rather than the one where $p_1^\mu = (M,0,0,0)$. In this frame we have $q^\mu = (0,\boldsymbol{q})$ and

$$\gamma = \sigma + \mathcal{O}(\boldsymbol{q}^2) = y + \mathcal{O}(\boldsymbol{q}^2)\,, \tag{4.23}$$

where γ is defined below eq. (3.8) and may also be expressed as $\gamma = v\cdot p_2/m$, $\sigma = p_1\cdot p_2/(mM)$ and $y = \bar{p}_1\cdot\bar{p}_2/(\bar{m}\bar{M})$ with $\bar{p}_2 = p_2 - \frac{1}{2}q$ and $\bar{m}^2 = \bar{p}_2^2$. Interestingly, we find that the

JHEP03(2024)125

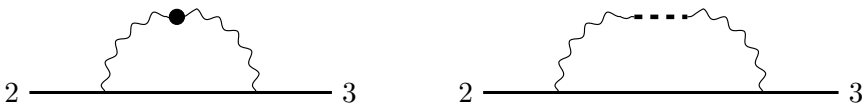

Figure 7. The Feynman diagrams that contribute to the 1SF amplitude at $\mathcal{O}\left(G^2\right)$. The external probe-particle lines have momenta p_2 and p_3.

barred variables introduced in ref. [98], which simplify amplitudes calculations relevant for gravitational-wave physics, naturally appear in our curved-space formalism.

We may make an interesting observation by studying the contribution of the background insertion and that of the deflection separately. The Compton amplitude is invariant under the transformation

$$\varepsilon_6 \to \varepsilon_6 + \lambda_6\, q_6\,, \quad \varepsilon_7 \to \varepsilon_7 + \lambda_7\, q_7\,, \tag{4.24}$$

for any (λ_6, λ_7). We may think of this as residual gauge freedom at the level of the amplitude and we may use it to simplify its form. In particular, if we choose (λ_6, λ_7) such that

$$v \cdot \varepsilon_6^* = 0\,, \quad v \cdot \varepsilon_7^* = 0\,, \tag{4.25}$$

where $\varepsilon_{6,7}^*$ signifies the corresponding gauge-fixed polarization, then we have

$$\mathcal{A}_{\rm C}^{\rm d} = 0\,, \quad \mathcal{A}_{\rm C} = \mathcal{A}_{\rm C}^{\rm b} = -\frac{8\pi G M\omega^2}{q_6 \cdot q_7}(\varepsilon_6^* \cdot \varepsilon_7^*)^2\,. \tag{4.26}$$

Given this result, one might wonder whether there exists a gauge choice such that the deflection part of the action never contributes, or whether this is an accident due to the simplicity of the particular example. By inspecting $S_{\rm H,\,FI}$ in eq. (4.15) we see that, while for all terms linear in z^μ there is at least one index of $h_{\mu\nu}$ contracted against v^μ, this stops being the case at quadratic order in z^μ. This suggests that the gauge choice in eq. (4.25) would not completely remove the deflection terms when quadratic-in-z^μ vertices become important. Nevertheless, it would be interesting to understand the extent to which gauge choices of this sort can simplify computations.

Finally, we compute the 1SF amplitude at $\mathcal{O}\left(G^2\right)$ via the Feynman diagrams depicted in figure 7. We also obtained the result via the generalized unitarity method [108, 109]. Our Compton amplitude satisfies the generalized Ward identity, hence we may use the de Donder projector when performing the sewing [110]. After some simple integral reduction and integration we find

$$\mathcal{A}_2^{\rm 1SF,\,\mathcal{O}\left(G^2\right)} = \frac{3\pi^2 G^2 M m^3 (5\gamma^2 - 1)}{|q|}\,, \tag{4.27}$$

where γ and q are defined below eqs. (3.8) and (4.22) respectively. This amplitude agrees with the familiar flat-space result [81, 92] up to non-relativistic normalization.

The complete $\mathcal{O}\left(G^2\right)$ amplitude is given by the Fourier transform of the second term in eq. (3.16) together with the one in eq. (4.27). While the total amplitude with appropriate normalization is symmetric under $m \leftrightarrow M$ exchange, we see that the contributions at 0SF and 1SF are obtained in quite different ways in our formalism.

JHEP03(2024)125

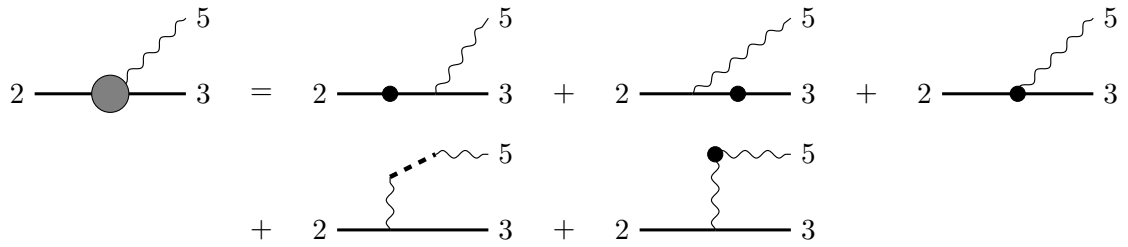

Figure 8. The single-graviton-emission amplitude given as a sum of Feynman diagrams. The gray large blob stands for the on-shell amplitude, while the rest of the symbols are defined in earlier figures. The on-shell graviton has momentum q_5 and polarization tensor ε_5. The probe-particle external lines have momenta p_2 and p_3.

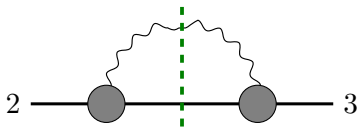

Figure 9. The unitarity cut from which we extract the integrand of the 1SF amplitude at $\mathcal{O}\left(G^3\right)$. The gray large blob stands for the on-shell amplitude we computed above. The vertical green dashed line signifies the unitarity cut, implying that the cut lines are taken on shell. The probe-particle external lines have momenta p_2 and p_3.

4.7 1SF amplitude at $\mathcal{O}\left(G^3\right)$

In this subsection we discuss our computation of the three-point single-graviton-emission amplitude, which corresponds to the flat-space five-point amplitude, and the integrand for the conservative 1SF amplitude at $\mathcal{O}\left(G^3\right)$ or 3PM.

The necessary Feynman diagrams for the single-graviton-emission amplitude are shown in figure 8. While the vertices with background insertions contain all-orders-in-G information, for the case at hand we may truncate them to leading order. At this order, the vertices arising from $S_{\rm L}$ and $S_{\rm LY}$ are identical. Similar to the Compton amplitude computed in the previous subsection, we find that for the polarization choice $v \cdot \varepsilon_5^* = 0$ the deflection contributions vanish in the classical limit.

Our amplitude matches the classical limit of the flat-space five-point amplitude obtained in ref. [83]. Our curved-space amplitude contains superclassical terms associated with the probe particle, which we may keep track of by formally considering complex kinematics. These are contained in the first two diagrams on the right hand side of the equation depicted in figure 8, and match the corresponding terms in the flat-space amplitude. On the other hand, our curved-space amplitudes do not contain superclassical terms associated with the heavy source.

We now turn to the 1SF amplitude at $\mathcal{O}\left(G^3\right)$. We build a generalized-unitarity [108, 109] integrand by sewing two single-graviton-emission amplitudes as in figure 9. The simplifications of ref. [110] are automatic in this case, given that we are sewing amplitudes with a single graviton. By taking further cuts we verify that we retrieve the unitarity cuts used to obtain the Hamiltonian at $\mathcal{O}\left(G^3\right)$ in ref. [82]. In particular, we obtain the so-called N and H cuts, which are relevant for the 1SF part of the amplitude at $\mathcal{O}\left(G^3\right)$. This provides a non-trivial validation of our formalism.

JHEP03(2024)125

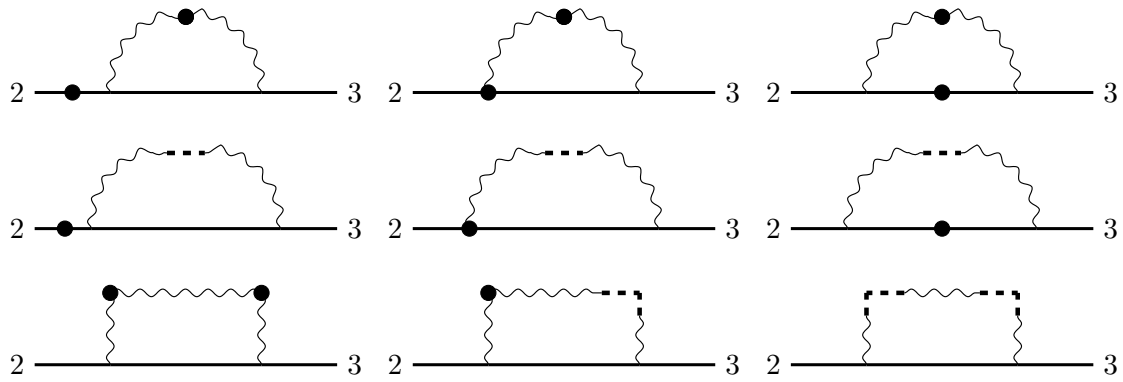

Figure 10. The Feynman diagrams that contribute to the 1SF amplitude at $\mathcal{O}\left(G^3\right)$. The probe-particle external lines have momenta p_2 and p_3. For the diagrams that are not $2 \leftrightarrow 3$ symmetric, one needs to add corresponding ones arising from $2 \leftrightarrow 3$ exchange.

Recently, ref. [77] computed the single-graviton-emission amplitude by solving the equations of motion for the probe particle and the graviton in the linearized Schwarzschild background. Their analysis employs restricted kinematics where recoil terms do not contribute. However, in a generic gauge, the construction of the 1SF amplitude at $\mathcal{O}\left(G^3\right)$ via unitarity would require recoil terms.

Alternatively, we also obtain an integrand for the 1SF amplitude at $\mathcal{O}\left(G^3\right)$ using the curved-space Feynman rules. We depict the relevant diagrams in figure 10. As mentioned above, the background vertices may be truncated to linear order in G. Also, in accordance with our general discussion in section 4.5, the last diagram in figure 10 does not contribute in the potential region. We verify the validity of this integrand in the same way as above.

5 Conclusions

In this paper we used EFT methods and scattering amplitudes in curved space to develop a framework for computing gravitational self-force corrections to binary dynamics, including the effects of the backreaction of the background spacetime. We explicitly verified a number of results, namely the 0SF two-point amplitude to all orders in G, the Compton and single-graviton-emission tree-level amplitudes, the 1SF two-point amplitude at $\mathcal{O}\left(G^2\right)$, and the integrand for the 1SF two-point amplitude at $\mathcal{O}\left(G^3\right)$. We find agreement with the literature in all cases.

In our setup, vertices encode information to all orders in G through the background metric, and perturbation theory is organized so that the loop expansion coincides with the SF expansion. Moreover, classes of higher-loop diagrams in flat space are mapped to a few lower-loop diagrams in curved space, which may reduce the number of integrations and automatically incorporate simplifications that would otherwise require non-trivial combinations of diagrams [111]. We depict an example of this feature in figure 11, where a family of flat-space diagrams are captured by the background insertion. For instance, a subclass of contributions to the 1SF amplitude and to all orders in G can be obtained as a one-loop computation through the top right of figure 11.

In the future, it would be interesting to consider a Kerr black hole as well as a spinning probe particle. Our formalism can also be applied for computing contributions at higher

JHEP03(2024)125

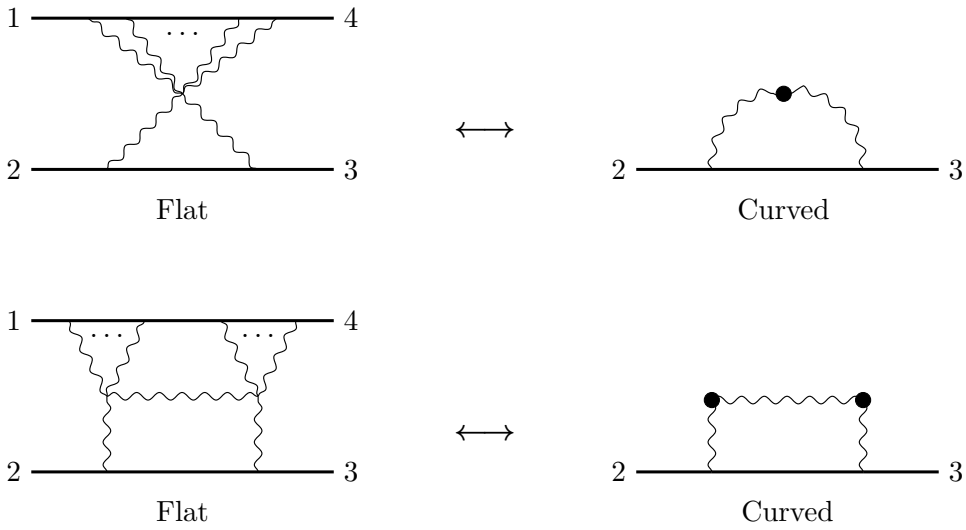

Figure 11. Schematic correspondence between classes of diagrams in a flat-space framework and the curved-space framework of this paper. In the top line, a multi-loop integral on the left is related to a one-loop integral on the right. In the bottom line, a multi-loop integral on the left is related to a two-loop integral on the right. See section 4.5 for a discussion of the integral vs diagram loop counting in the curved-space formalism.

SF order and at higher order in G. For example, one could target the 1SF terms at $\mathcal{O}(G^5)$ as a first pass at 5PM. Radiative effects constitute another natural target; these may be addressed for example by adopting ideas from the amplitudes approach of ref. [112], as in, e.g., refs. [113, 114], or from the "in-in" or "closed-time-path" formalism [115–117], as in, e.g., refs. [23, 39, 118–121]. In pursuing such calculations, it would be advantageous to incorporate on-shell methods or to further simplify perturbation theory by choosing special gauges. It would be interesting to see if the advantages of curved-space amplitudes can help with the complexity of calculations at higher PM orders.

Finally, many aspects of our analysis are still anchored to properties of amplitudes in flat space, and it would be interesting to explore alternative methods of calculation that are instead tailored to the inherent properties of amplitudes in curved space. For example, the all-orders-in-G position-space amplitude in eq. (3.14) is compact, and suggests that one might calculate in position space where metrics are naturally expressed. Another example is our deference to the flat-space propagator; one might instead consider numerical methods for evaluating Green's functions in curved space.

Acknowledgments

We are especially grateful to Carl Beadle, Clifford Cheung, Michael Ruf, Fei Teng and Chia-Hsien Shen. We also wish to thank Zvi Bern, Andrea Cristofoli, Callum Jones, Davide Perrone, Sergio Ricossa, Francesco Riva, Radu Roiban and Francesco Serra. The work of D. K. is supported by the Swiss National Science Foundation under grant no. 200021-205016. The work of M. S. is supported by the US Department of Energy Early Career program under award number DE-SC0024224, and the Sloan Foundation. We are also grateful to the Mani L. Bhaumik Institute for Theoretical Physics for support.

JHEP03(2024)125

References

[1] LIGO Scientific and Virgo collaborations, *Observation of Gravitational Waves from a Binary Black Hole Merger*, *Phys. Rev. Lett.* **116** (2016) 061102 [arXiv:1602.03837] [INSPIRE].

[2] A. Buonanno et al., *Snowmass White Paper: Gravitational Waves and Scattering Amplitudes*, in the proceedings of the *Snowmass 2021*, Seattle, U.S.A., July 17–26 (2022) [arXiv:2204.05194] [INSPIRE].

[3] T. Adamo et al., *Snowmass White Paper: the Double Copy and its Applications*, in the proceedings of the *Snowmass 2021*, Seattle, U.S.A., July 17–26 (2022) [arXiv:2204.06547] [INSPIRE].

[4] N.E.J. Bjerrum-Bohr, P.H. Damgaard, L. Planté and P. Vanhove, *The SAGEX review on scattering amplitudes Chapter 13: Post-Minkowskian expansion from scattering amplitudes*, *J. Phys. A* **55** (2022) 443014 [arXiv:2203.13024] [INSPIRE].

[5] D.A. Kosower, R. Monteiro and D. O'Connell, *The SAGEX review on scattering amplitudes Chapter 14: Classical gravity from scattering amplitudes*, *J. Phys. A* **55** (2022) 443015 [arXiv:2203.13025] [INSPIRE].

[6] LISA collaboration, *Laser Interferometer Space Antenna*, arXiv:1702.00786 [INSPIRE].

[7] M. Punturo et al., *The Einstein Telescope: A third-generation gravitational wave observatory*, *Class. Quant. Grav.* **27** (2010) 194002 [INSPIRE].

[8] D. Reitze et al., *Cosmic Explorer: The U.S. Contribution to Gravitational-Wave Astronomy beyond LIGO*, *Bull. Am. Astron. Soc.* **51** (2019) 035 [arXiv:1907.04833] [INSPIRE].

[9] H. Kawai, D.C. Lewellen and S.H.H. Tye, *A Relation Between Tree Amplitudes of Closed and Open Strings*, *Nucl. Phys. B* **269** (1986) 1 [INSPIRE].

[10] Z. Bern, J.J.M. Carrasco and H. Johansson, *New Relations for Gauge-Theory Amplitudes*, *Phys. Rev. D* **78** (2008) 085011 [arXiv:0805.3993] [INSPIRE].

[11] Z. Bern, J.J.M. Carrasco and H. Johansson, *Perturbative Quantum Gravity as a Double Copy of Gauge Theory*, *Phys. Rev. Lett.* **105** (2010) 061602 [arXiv:1004.0476] [INSPIRE].

[12] Z. Bern et al., *The Duality Between Color and Kinematics and its Applications*, arXiv:1909.01358 [INSPIRE].

[13] C. Cheung, N. Shah and M.P. Solon, *Mining the Geodesic Equation for Scattering Data*, *Phys. Rev. D* **103** (2021) 024030 [arXiv:2010.08568] [INSPIRE].

[14] A. Cristofoli et al., *The Uncertainty Principle and Classical Amplitudes*, arXiv:2112.07556 [INSPIRE].

[15] Z. Bern et al., *Scattering Amplitudes and Conservative Binary Dynamics at $\mathcal{O}(G^4)$*, *Phys. Rev. Lett.* **126** (2021) 171601 [arXiv:2101.07254] [INSPIRE].

[16] L. Blanchet, *Gravitational Radiation from Post-Newtonian Sources and Inspiralling Compact Binaries*, *Living Rev. Rel.* **17** (2014) 2 [arXiv:1310.1528] [INSPIRE].

[17] W.D. Goldberger and I.Z. Rothstein, *An effective field theory of gravity for extended objects*, *Phys. Rev. D* **73** (2006) 104029 [hep-th/0409156] [INSPIRE].

JHEP03(2024)125

[18] R.A. Porto, *The effective field theorist's approach to gravitational dynamics*, *Phys. Rept.* **633** (2016) 1 [arXiv:1601.04914] [INSPIRE].

[19] M. Levi, *Effective Field Theories of Post-Newtonian Gravity: A comprehensive review*, *Rept. Prog. Phys.* **83** (2020) 075901 [arXiv:1807.01699] [INSPIRE].

[20] Z. Bern et al., *Scattering Amplitudes, the Tail Effect, and Conservative Binary Dynamics at O(G4)*, *Phys. Rev. Lett.* **128** (2022) 161103 [arXiv:2112.10750] [INSPIRE].

[21] C. Dlapa, G. Kälin, Z. Liu and R.A. Porto, *Dynamics of binary systems to fourth Post-Minkowskian order from the effective field theory approach*, *Phys. Lett. B* **831** (2022) 137203 [arXiv:2106.08276] [INSPIRE].

[22] C. Dlapa, G. Kälin, Z. Liu and R.A. Porto, *Conservative Dynamics of Binary Systems at Fourth Post-Minkowskian Order in the Large-Eccentricity Expansion*, *Phys. Rev. Lett.* **128** (2022) 161104 [arXiv:2112.11296] [INSPIRE].

[23] C. Dlapa et al., *Radiation Reaction and Gravitational Waves at Fourth Post-Minkowskian Order*, *Phys. Rev. Lett.* **130** (2023) 101401 [arXiv:2210.05541] [INSPIRE].

[24] P.H. Damgaard, E.R. Hansen, L. Planté and P. Vanhove, *Classical observables from the exponential representation of the gravitational S-matrix*, *JHEP* **09** (2023) 183 [arXiv:2307.04746] [INSPIRE].

[25] G.U. Jakobsen et al., *Conservative Scattering of Spinning Black Holes at Fourth Post-Minkowskian Order*, *Phys. Rev. Lett.* **131** (2023) 151401 [arXiv:2306.01714] [INSPIRE].

[26] Y. Mino, M. Sasaki and T. Tanaka, *Gravitational radiation reaction to a particle motion*, *Phys. Rev. D* **55** (1997) 3457 [gr-qc/9606018] [INSPIRE].

[27] T.C. Quinn and R.M. Wald, *An axiomatic approach to electromagnetic and gravitational radiation reaction of particles in curved space-time*, *Phys. Rev. D* **56** (1997) 3381 [gr-qc/9610053] [INSPIRE].

[28] S.L. Detweiler, *Radiation reaction and the selfforce for a point mass in general relativity*, *Phys. Rev. Lett.* **86** (2001) 1931 [gr-qc/0011039] [INSPIRE].

[29] S.L. Detweiler and B.F. Whiting, *Selfforce via a Green's function decomposition*, *Phys. Rev. D* **67** (2003) 024025 [gr-qc/0202086] [INSPIRE].

[30] S.E. Gralla and R.M. Wald, *A Rigorous Derivation of Gravitational Self-force*, *Class. Quant. Grav.* **25** (2008) 205009 [*Erratum ibid.* **28** (2011) 159501] [arXiv:0806.3293] [INSPIRE].

[31] A. Pound, *Self-consistent gravitational self-force*, *Phys. Rev. D* **81** (2010) 024023 [arXiv:0907.5197] [INSPIRE].

[32] E. Rosenthal, *Second-order gravitational self-force*, *Phys. Rev. D* **74** (2006) 084018 [gr-qc/0609069] [INSPIRE].

[33] S. Detweiler, *Gravitational radiation reaction and second order perturbation theory*, *Phys. Rev. D* **85** (2012) 044048 [arXiv:1107.2098] [INSPIRE].

[34] A. Pound, *Second-order gravitational self-force*, *Phys. Rev. Lett.* **109** (2012) 051101 [arXiv:1201.5089] [INSPIRE].

[35] S.E. Gralla, *Second Order Gravitational Self Force*, *Phys. Rev. D* **85** (2012) 124011 [arXiv:1203.3189] [INSPIRE].

[36] L. Barack and A. Pound, *Self-force and radiation reaction in general relativity*, *Rept. Prog. Phys.* **82** (2019) 016904 [arXiv:1805.10385] [INSPIRE].

JHEP03(2024)125

[37] A. Pound and B. Wardell, *Black hole perturbation theory and gravitational self-force*, arXiv:2101.04592 [DOI:10.1007/978-981-15-4702-7_38-1] [INSPIRE].

[38] C.R. Galley, B.L. Hu and S.-Y. Lin, *Electromagnetic and gravitational self-force on a relativistic particle from quantum fields in curved space*, *Phys. Rev. D* **74** (2006) 024017 [gr-qc/0603099] [INSPIRE].

[39] C.R. Galley and B.L. Hu, *Self-force on extreme mass ratio inspirals via curved spacetime effective field theory*, *Phys. Rev. D* **79** (2009) 064002 [arXiv:0801.0900] [INSPIRE].

[40] T. Hinderer and E.E. Flanagan, *Two timescale analysis of extreme mass ratio inspirals in Kerr. I. Orbital Motion*, *Phys. Rev. D* **78** (2008) 064028 [arXiv:0805.3337] [INSPIRE].

[41] S. Isoyama et al., *Impact of the second-order self-forces on the dephasing of the gravitational waves from quasicircular extreme mass-ratio inspirals*, *Phys. Rev. D* **87** (2013) 024010 [arXiv:1210.2569] [INSPIRE].

[42] L.M. Burko and G. Khanna, *Self-force gravitational waveforms for extreme and intermediate mass ratio inspirals. II: Importance of the second-order dissipative effect*, *Phys. Rev. D* **88** (2013) 024002 [arXiv:1304.5296] [INSPIRE].

[43] L. Barack and N. Sago, *Gravitational self-force on a particle in eccentric orbit around a Schwarzschild black hole*, *Phys. Rev. D* **81** (2010) 084021 [arXiv:1002.2386] [INSPIRE].

[44] L. Barack and N. Sago, *Beyond the geodesic approximation: conservative effects of the gravitational self-force in eccentric orbits around a Schwarzschild black hole*, *Phys. Rev. D* **83** (2011) 084023 [arXiv:1101.3331] [INSPIRE].

[45] B. Wardell et al., *Gravitational Waveforms for Compact Binaries from Second-Order Self-Force Theory*, *Phys. Rev. Lett.* **130** (2023) 241402 [arXiv:2112.12265] [INSPIRE].

[46] S.E. Gralla and K. Lobo, *Self-force effects in post-Minkowskian scattering*, *Class. Quant. Grav.* **39** (2022) 095001 [arXiv:2110.08681] [INSPIRE].

[47] L. Barack and O. Long, *Self-force correction to the deflection angle in black-hole scattering: A scalar charge toy model*, *Phys. Rev. D* **106** (2022) 104031 [arXiv:2209.03740] [INSPIRE].

[48] L. Barack et al., *Comparison of post-Minkowskian and self-force expansions: Scattering in a scalar charge toy model*, *Phys. Rev. D* **108** (2023) 024025 [arXiv:2304.09200] [INSPIRE].

[49] M.J. Duff, *Quantum Tree Graphs and the Schwarzschild Solution*, *Phys. Rev. D* **7** (1973) 2317 [INSPIRE].

[50] D. Neill and I.Z. Rothstein, *Classical Space-Times from the S Matrix*, *Nucl. Phys. B* **877** (2013) 177 [arXiv:1304.7263] [INSPIRE].

[51] S. Mougiakakos and P. Vanhove, *Schwarzschild-Tangherlini metric from scattering amplitudes in various dimensions*, *Phys. Rev. D* **103** (2021) 026001 [arXiv:2010.08882] [INSPIRE].

[52] G.U. Jakobsen, *Schwarzschild-Tangherlini Metric from Scattering Amplitudes*, *Phys. Rev. D* **102** (2020) 104065 [arXiv:2006.01734] [INSPIRE].

[53] S. D'Onofrio, F. Fragomeno, C. Gambino and F. Riccioni, *The Reissner-Nordström-Tangherlini solution from scattering amplitudes of charged scalars*, *JHEP* **09** (2022) 013 [arXiv:2207.05841] [INSPIRE].

[54] N. Siemonsen and J. Vines, *Test black holes, scattering amplitudes and perturbations of Kerr spacetime*, *Phys. Rev. D* **101** (2020) 064066 [arXiv:1909.07361] [INSPIRE].

[55] A. Guevara, A. Ochirov and J. Vines, *Black-hole scattering with general spin directions from minimal-coupling amplitudes*, *Phys. Rev. D* **100** (2019) 104024 [arXiv:1906.10071] [INSPIRE].

JHEP03(2024)125

[56] A. Guevara, A. Ochirov and J. Vines, *Scattering of Spinning Black Holes from Exponentiated Soft Factors*, *JHEP* **09** (2019) 056 [arXiv:1812.06895] [INSPIRE].

[57] M.-Z. Chung, Y.-T. Huang, J.-W. Kim and S. Lee, *The simplest massive S-matrix: from minimal coupling to Black Holes*, *JHEP* **04** (2019) 156 [arXiv:1812.08752] [INSPIRE].

[58] M.-Z. Chung, Y.-T. Huang and J.-W. Kim, *Classical potential for general spinning bodies*, *JHEP* **09** (2020) 074 [arXiv:1908.08463] [INSPIRE].

[59] M.-Z. Chung, Y.-T. Huang, J.-W. Kim and S. Lee, *Complete Hamiltonian for spinning binary systems at first post-Minkowskian order*, *JHEP* **05** (2020) 105 [arXiv:2003.06600] [INSPIRE].

[60] W.-M. Chen, M.-Z. Chung, Y.-T. Huang and J.-W. Kim, *The 2PM Hamiltonian for binary Kerr to quartic in spin*, *JHEP* **08** (2022) 148 [arXiv:2111.13639] [INSPIRE].

[61] N. Arkani-Hamed, Y.-T. Huang and D. O'Connell, *Kerr black holes as elementary particles*, *JHEP* **01** (2020) 046 [arXiv:1906.10100] [INSPIRE].

[62] Z. Bern et al., *Spinning black hole binary dynamics, scattering amplitudes, and effective field theory*, *Phys. Rev. D* **104** (2021) 065014 [arXiv:2005.03071] [INSPIRE].

[63] D. Kosmopoulos and A. Luna, *Quadratic-in-spin Hamiltonian at $\mathcal{O}(G^2)$ from scattering amplitudes*, *JHEP* **07** (2021) 037 [arXiv:2102.10137] [INSPIRE].

[64] Z. Bern et al., *Binary Dynamics through the Fifth Power of Spin at $\mathcal{O}(G^2)$*, *Phys. Rev. Lett.* **130** (2023) 201402 [arXiv:2203.06202] [INSPIRE].

[65] R. Aoude, K. Haddad and A. Helset, *On-shell heavy particle effective theories*, *JHEP* **05** (2020) 051 [arXiv:2001.09164] [INSPIRE].

[66] R. Aoude, K. Haddad and A. Helset, *Searching for Kerr in the 2PM amplitude*, *JHEP* **07** (2022) 072 [arXiv:2203.06197] [INSPIRE].

[67] R. Aoude, K. Haddad and A. Helset, *Classical gravitational scattering amplitude at $\mathcal{O}(G^2 S_1^\infty S_2^\infty)$*, *Phys. Rev. D* **108** (2023) 024050 [arXiv:2304.13740] [INSPIRE].

[68] R. Aoude, K. Haddad and A. Helset, *Classical Gravitational Spinning-Spinless Scattering at $\mathcal{O}(G^2 S^\infty)$*, *Phys. Rev. Lett.* **129** (2022) 141102 [arXiv:2205.02809] [INSPIRE].

[69] B. Maybee, D. O'Connell and J. Vines, *Observables and amplitudes for spinning particles and black holes*, *JHEP* **12** (2019) 156 [arXiv:1906.09260] [INSPIRE].

[70] N.E.J. Bjerrum-Bohr, G. Chen and M. Skowronek, *Classical spin gravitational Compton scattering*, *JHEP* **06** (2023) 170 [arXiv:2302.00498] [INSPIRE].

[71] T. Adamo and A. Ilderton, *Classical and quantum double copy of back-reaction*, *JHEP* **09** (2020) 200 [arXiv:2005.05807] [INSPIRE].

[72] A. Cristofoli, *Gravitational shock waves and scattering amplitudes*, *JHEP* **11** (2020) 160 [arXiv:2006.08283] [INSPIRE].

[73] T. Adamo, A. Cristofoli and P. Tourkine, *Eikonal amplitudes from curved backgrounds*, *SciPost Phys.* **13** (2022) 032 [arXiv:2112.09113] [INSPIRE].

[74] T. Adamo, L. Mason and A. Sharma, *Graviton scattering in self-dual radiative space-times*, *Class. Quant. Grav.* **40** (2023) 095002 [arXiv:2203.02238] [INSPIRE].

[75] T. Adamo, A. Cristofoli and A. Ilderton, *Classical physics from amplitudes on curved backgrounds*, *JHEP* **08** (2022) 281 [arXiv:2203.13785] [INSPIRE].

[76] T. Adamo, A. Cristofoli, A. Ilderton and S. Klisch, *All Order Gravitational Waveforms from Scattering Amplitudes*, *Phys. Rev. Lett.* **131** (2023) 011601 [arXiv:2210.04696] [INSPIRE].

JHEP03(2024)125

[77] T. Adamo, A. Cristofoli, A. Ilderton and S. Klisch, *Scattering amplitudes for self-force*, *Class. Quant. Grav.* **41** (2024) 065006 [arXiv:2307.00431] [INSPIRE].

[78] I. Low and A.V. Manohar, *Spontaneously broken space-time symmetries and Goldstone's theorem*, *Phys. Rev. Lett.* **88** (2002) 101602 [hep-th/0110285] [INSPIRE].

[79] H. Watanabe and H. Murayama, *Redundancies in Nambu-Goldstone Bosons*, *Phys. Rev. Lett.* **110** (2013) 181601 [arXiv:1302.4800] [INSPIRE].

[80] L.V. Delacrétaz et al., *(Re-)Inventing the Relativistic Wheel: Gravity, Cosets, and Spinning Objects*, *JHEP* **11** (2014) 008 [arXiv:1405.7384] [INSPIRE].

[81] N.E.J. Bjerrum-Bohr, J.F. Donoghue and B.R. Holstein, *Quantum gravitational corrections to the nonrelativistic scattering potential of two masses*, *Phys. Rev. D* **67** (2003) 084033 [*Erratum ibid.* **71** (2005) 069903] [hep-th/0211072] [INSPIRE].

[82] Z. Bern et al., *Scattering Amplitudes and the Conservative Hamiltonian for Binary Systems at Third Post-Minkowskian Order*, *Phys. Rev. Lett.* **122** (2019) 201603 [arXiv:1901.04424] [INSPIRE].

[83] A. Luna, I. Nicholson, D. O'Connell and C.D. White, *Inelastic Black Hole Scattering from Charged Scalar Amplitudes*, *JHEP* **03** (2018) 044 [arXiv:1711.03901] [INSPIRE].

[84] C. Cheung et al., *Effective Field Theory for Extreme Mass Ratio Binaries*, *Phys. Rev. Lett.* **132** (2024) 091402 [arXiv:2308.14832] [INSPIRE].

[85] N.D. Birrell and P.C.W. Davies, *Quantum Fields in Curved Space*, Cambridge Univ. Press, Cambridge, U.K. (1984) [DOI:10.1017/CBO9780511622632] [INSPIRE].

[86] L.E. Parker and D. Toms, *Quantum Field Theory in Curved Spacetime: Quantized Field and Gravity*, Cambridge University Press (2009) [DOI:10.1017/CBO9780511813924] [INSPIRE].

[87] R.M. Wald, *On Particle Creation by Black Holes*, *Commun. Math. Phys.* **45** (1975) 9 [INSPIRE].

[88] L. Parker, *Probability Distribution of Particles Created by a Black Hole*, *Phys. Rev. D* **12** (1975) 1519 [INSPIRE].

[89] S.W. Hawking, *Particle Creation by Black Holes*, *Commun. Math. Phys.* **43** (1975) 199 [*Erratum ibid.* **46** (1976) 206] [INSPIRE].

[90] F.R. Tangherlini, *Schwarzschild field in n dimensions and the dimensionality of space problem*, *Nuovo Cim.* **27** (1963) 636 [INSPIRE].

[91] I. Komissarov, A. Nicolis and J. Staunton, *Cosmology as a weak gravitational field and the trans-Planckian problem*, *JHEP* **05** (2023) 216 [arXiv:2210.11508] [INSPIRE].

[92] C. Cheung, I.Z. Rothstein and M.P. Solon, *From Scattering Amplitudes to Classical Potentials in the Post-Minkowskian Expansion*, *Phys. Rev. Lett.* **121** (2018) 251101 [arXiv:1808.02489] [INSPIRE].

[93] G. Kälin and R.A. Porto, *From Boundary Data to Bound States*, *JHEP* **01** (2020) 072 [arXiv:1910.03008] [INSPIRE].

[94] Z. Bern et al., *Black Hole Binary Dynamics from the Double Copy and Effective Theory*, *JHEP* **10** (2019) 206 [arXiv:1908.01493] [INSPIRE].

[95] M.B. Wise, *Chiral perturbation theory for hadrons containing a heavy quark*, *Phys. Rev. D* **45** (1992) R2188 [INSPIRE].

[96] P.H. Damgaard, K. Haddad and A. Helset, *Heavy Black Hole Effective Theory*, *JHEP* **11** (2019) 070 [arXiv:1908.10308] [INSPIRE].

JHEP03(2024)125

[97] J. Heinonen, R.J. Hill and M.P. Solon, *Lorentz invariance in heavy particle effective theories*, *Phys. Rev. D* **86** (2012) 094020 [arXiv:1208.0601] [INSPIRE].

[98] J. Parra-Martinez, M.S. Ruf and M. Zeng, *Extremal black hole scattering at $\mathcal{O}(G^3)$: graviton dominance, eikonal exponentiation, and differential equations*, *JHEP* **11** (2020) 023 [arXiv:2005.04236] [INSPIRE].

[99] V. Balasubramanian, B. Craps, M. De Clerck and K. Nguyen, *Superluminal chaos after a quantum quench*, *JHEP* **12** (2019) 132 [arXiv:1908.08955] [INSPIRE].

[100] U. Kol, D. O'connell and O. Telem, *The radial action from probe amplitudes to all orders*, *JHEP* **03** (2022) 141 [arXiv:2109.12092] [INSPIRE].

[101] S. Kim, P. Kraus, R. Monten and R.M. Myers, *S-matrix path integral approach to symmetries and soft theorems*, *JHEP* **10** (2023) 036 [arXiv:2307.12368] [INSPIRE].

[102] J. Polchinski, *String theory. Volume 1: An introduction to the bosonic string*, Cambridge University Press (2007) [DOI:10.1017/CBO9780511816079] [INSPIRE].

[103] G. Mogull, J. Plefka and J. Steinhoff, *Classical black hole scattering from a worldline quantum field theory*, *JHEP* **02** (2021) 048 [arXiv:2010.02865] [INSPIRE].

[104] R.A. Porto, *Post-Newtonian corrections to the motion of spinning bodies in NRGR*, *Phys. Rev. D* **73** (2006) 104031 [gr-qc/0511061] [INSPIRE].

[105] G. Kälin and R.A. Porto, *Post-Minkowskian Effective Field Theory for Conservative Binary Dynamics*, *JHEP* **11** (2020) 106 [arXiv:2006.01184] [INSPIRE].

[106] Z. Liu, R.A. Porto and Z. Yang, *Spin Effects in the Effective Field Theory Approach to Post-Minkowskian Conservative Dynamics*, *JHEP* **06** (2021) 012 [arXiv:2102.10059] [INSPIRE].

[107] R.P. Geroch and J.H. Traschen, *Strings and Other Distributional Sources in General Relativity*, *Conf. Proc. C* **861214** (1986) 138 [INSPIRE].

[108] Z. Bern, L.J. Dixon, D.C. Dunbar and D.A. Kosower, *One loop n point gauge theory amplitudes, unitarity and collinear limits*, *Nucl. Phys. B* **425** (1994) 217 [hep-ph/9403226] [INSPIRE].

[109] Z. Bern, L.J. Dixon, D.C. Dunbar and D.A. Kosower, *Fusing gauge theory tree amplitudes into loop amplitudes*, *Nucl. Phys. B* **435** (1995) 59 [hep-ph/9409265] [INSPIRE].

[110] D. Kosmopoulos, *Simplifying D-dimensional physical-state sums in gauge theory and gravity*, *Phys. Rev. D* **105** (2022) 056025 [arXiv:2009.00141] [INSPIRE].

[111] R. Akhoury, R. Saotome and G. Sterman, *High Energy Scattering in Perturbative Quantum Gravity at Next to Leading Power*, *Phys. Rev. D* **103** (2021) 064036 [arXiv:1308.5204] [INSPIRE].

[112] D.A. Kosower, B. Maybee and D. O'Connell, *Amplitudes, Observables, and Classical Scattering*, *JHEP* **02** (2019) 137 [arXiv:1811.10950] [INSPIRE].

[113] E. Herrmann, J. Parra-Martinez, M.S. Ruf and M. Zeng, *Gravitational Bremsstrahlung from Reverse Unitarity*, *Phys. Rev. Lett.* **126** (2021) 201602 [arXiv:2101.07255] [INSPIRE].

[114] E. Herrmann, J. Parra-Martinez, M.S. Ruf and M. Zeng, *Radiative classical gravitational observables at $\mathcal{O}(G^3)$ from scattering amplitudes*, *JHEP* **10** (2021) 148 [arXiv:2104.03957] [INSPIRE].

[115] J.S. Schwinger, *Brownian motion of a quantum oscillator*, *J. Math. Phys.* **2** (1961) 407 [INSPIRE].

JHEP03(2024)125

[116] L.V. Keldysh, *Diagram technique for nonequilibrium processes*, *Zh. Eksp. Teor. Fiz.* **47** (1964) 1515 [INSPIRE].

[117] E.A. Calzetta and B.-L.B. Hu, *Nonequilibrium Quantum Field Theory*, Oxford University Press (2009) [DOI:10.1017/9781009290036] [INSPIRE].

[118] A. Edison and M. Levi, *A tale of tails through generalized unitarity*, *Phys. Lett. B* **837** (2023) 137634 [arXiv:2202.04674] [INSPIRE].

[119] G.U. Jakobsen, G. Mogull, J. Plefka and B. Sauer, *All things retarded: radiation-reaction in worldline quantum field theory*, *JHEP* **10** (2022) 128 [arXiv:2207.00569] [INSPIRE].

[120] G.U. Jakobsen, G. Mogull, J. Plefka and B. Sauer, *Dissipative Scattering of Spinning Black Holes at Fourth Post-Minkowskian Order*, *Phys. Rev. Lett.* **131** (2023) 241402 [arXiv:2308.11514] [INSPIRE].

[121] G. Kälin, J. Neef and R.A. Porto, *Radiation-reaction in the Effective Field Theory approach to Post-Minkowskian dynamics*, *JHEP* **01** (2023) 140 [arXiv:2207.00580] [INSPIRE].

JHEP03(2024)125